A note on optimal transient growth in turbulent channel flows

Gregory Pujals,[1,2] Manuel García-Villalba,[3] Carlo Cossu,[1] and Sebastien Depardon[2]
[1]*LadHyX, CNRS-École Polytechnique, F-91128 Palaiseau, France*
[2]*PSA Peugeot Citroën, Centre Technique de Velizy, 2 Route de Gisy, 78943 Vélizy-Villacoublay Cedex, France*
[3]*Institute for Hydromechanics, University of Karlsruhe, D-76128 Karlsruhe, Germany*

(Received 13 June 2008; accepted 8 December 2008; published online 29 January 2009)

We compute the optimal transient growth of perturbations sustained by a turbulent channel flow following the same approach recently used by del Álamo and Jiménez [J. Fluid Mech. **559**, 205 (2006)]. Contrary to this previous analysis, we use generalized Orr–Sommerfeld and Squire operators consistent with previous investigations of mean flows with variable viscosity. The optimal perturbations are streamwise vortices evolving into streamwise streaks. In accordance with del Álamo and Jiménez, it is found that for very elongated structures and for sufficiently large Reynolds numbers, the optimal energy growth presents a primary peak in the spanwise wavelength, scaling in outer units, and a secondary peak scaling in inner units and corresponding to $\lambda_z^+ \approx 100$. Contrary to the previous results, however, it is found that the maximum energy growth associated with the primary peak increases with the Reynolds number. This growth, in a first approximation, scales linearly with an effective Reynolds number based on the centerline velocity, the channel half width and the maximum eddy viscosity associated. The optimal streaks associated with the primary peak have an optimal spacing of $\lambda_z = 4h$ and scale in outer units in the outer region and in wall units in the near wall region, where they still have up to 50% of their maximum amplitude near $y^+ = 10$. © *2009 American Institute of Physics*. [DOI: 10.1063/1.3068760]

I. INTRODUCTION

Streaky structures, i.e., narrow regions where the streamwise velocity is lower or larger than the mean, are very commonly observed in turbulent shear flows. It is well known[1,2] that such structures exist in the near wall region of turbulent boundary layers and channel flows where they scale in wall units with a mean spanwise spacing $\lambda_z^+ \approx 100$. There is also evidence of the existence of large coherent streaky structures extending outside the near wall region in the turbulent boundary layer,[3,4] the turbulent Couette flow,[5] and the turbulent channel flow.[6] The size of these structures seems to scale in external units.

In the case of laminar shear flows, it is known that streaks have the potential to be largely amplified from streamwise vortices through the lift-up effect.[7–9] The maximum energy growth leading to the most amplified streaks has been computed for virtually all the usual laminar shear flows.[10] In the case of the laminar channel flow, it has been found[11] that the optimal streaks are streamwise uniform with an optimal spanwise wavelength $\lambda_z \sim 3h$, where h is the channel half width.

Butler and Farrell[12] were the first to compute the optimally amplified streaks in the turbulent channel flow. They used the Reynolds–Tiederman[13] turbulent mean profile based on the Cess[14] eddy viscosity model but used the molecular viscosity in the linearized equations for the perturbations. They found the same optimal streak spacing as in the laminar case ($\lambda_z \sim 3h$), but they were able to retrieve the near wall streaks optimal spacing $\lambda_z^+ \approx 100$ only by constraining the optimization time to a fixed eddy turnover time. del Álamo and Jiménez[15] repeated the analysis using the eddy viscosity also in the equations for the perturbations. They found, without any constraint on the optimization time that the most amplified structures are elongated in the streamwise direction and that two peaks exist for the most amplified spanwise wavelength: a secondary one scaling in inner units and corresponding to $\lambda_z^+ \approx 100$ and a primary one scaling in outer units and with $\lambda_z \approx 3h$. However, contrary to the laminar case, the growth associated with this outer peak decreased when the Reynolds number was increased.

Further investigation, related to the computation of the optimal growth supported by a turbulent boundary layer,[16] revealed that the linearized equations for the perturbations used in Ref. 15 were not consistent with the ones used in previous linear stability analysis of turbulent mean flows[17] and of laminar flows with variable viscosity.[18] The scope of the present paper is, therefore, to repeat the analysis of del Álamo and Jiménez[15] for the turbulent channel flow using the linear operator consistent with previous investigations of the stability of turbulent and laminar flows with variable viscosity.[17,18] We anticipate that we find that the maximum transient growth associated with the outer peak increases with the Reynolds number. These revised results are consistent with experimental evidence that the energy contained in large scale streaky structures increases with the Reynolds number.

II. TURBULENT MEAN FLOW

We consider the statistically steady, parallel, and spanwise uniform turbulent flow of a viscous fluid in a plane channel of half width h. Modeling the turbulent shear stress with a turbulent eddy viscosity ν_t, and defining a total eddy

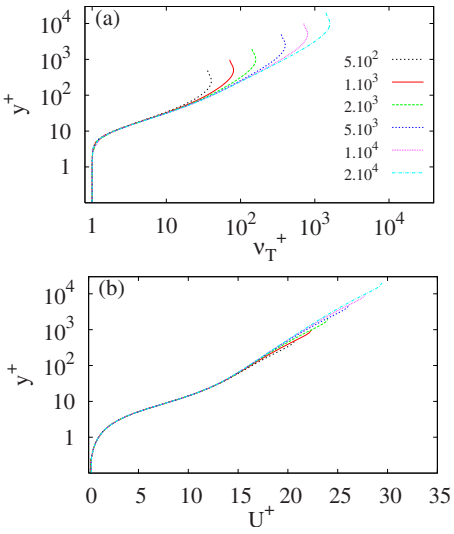

FIG. 1. (Color online) (a) Cess eddy viscosity ν_T^+ and (b) corresponding mean velocity profile, both displayed in wall units for the selected Reynolds numbers Re_τ=500, 1000, 2000, 5000, 10 000, and 20 000.

viscosity $\nu_T=\nu+\nu_t$, gives in dimensionless units: $Re_\tau\tau^+ = \nu_T^+(\eta)dU^+/d\eta$, where $\nu_T^+=\nu_T/\nu$, $\tau^+=\tau/(\rho u_\tau^2)$, $\mathrm{Re}_\tau=u_\tau h/\nu$ is the Reynolds number based on the friction velocity u_τ and the half width h of the channel; $\eta=y/h$. Cess[14] expression[19] for the total eddy viscosity is assumed as in previous studies,[15,17]

$$\nu_T^+(\eta)=\frac{1}{2}\left\{1+\frac{\kappa^2\,\mathrm{Re}_\tau^2}{9}(1-\eta^2)^2(1+2\eta^2)^2 \times\{1-\exp[(|\eta|-1)\mathrm{Re}_\tau/A]\}^2\right\}^{1/2}+\frac{1}{2}, \tag{1}$$

where the same values for the von Kármán constant κ =0.426 and the constant A=25.4 used in Ref. 15 will be used in the following. However, we have to remark that these constants have been fitted to direct numerical simulation (DNS) results[20] for Re_τ=2000 and that, therefore, the validity of this basic flow profile is dubious at very large Re_τ. Profiles of $\nu_T^+(\eta)$ are displayed in Fig. 1(a). The mean velocity profile can be retrieved by integrating $dU^+/d\eta$ $=-\mathrm{Re}_\tau\eta/\nu_T^+(\eta)$, as initially proposed by Reynolds and Tiedermann.[13] The mean velocity profiles corresponding to the ν_T^+ reported in Fig. 1(a) are displayed in Fig. 1(b) in inner units.

III. LINEARIZED EQUATIONS

Small perturbations $\mathbf{u}=(u,v,w)$, p to the turbulent mean flow $\mathbf{U}=[U(y),0,0]$ satisfy the continuity $\nabla\cdot\mathbf{u}=0$ and the linearized momentum equation,[17]

$$\frac{\partial\mathbf{u}}{\partial t}+U\frac{\partial\mathbf{u}}{\partial x}+(v\,\partial U/\partial y,0,0)=-\nabla p+\nabla\cdot[\nu_T(y)(\nabla\mathbf{u}+\nabla\mathbf{u}^T)]. \tag{2}$$

Perturbations of the form $\mathbf{u}(x,y,z,t)=\hat{\mathbf{u}}(\alpha,y,\beta,t)e^{i(\alpha x+\beta z)}$ are considered (due to the homogeneous nature of the mean flow in the horizontal plane), where α and β are the streamwise and spanwise wavenumbers, respectively. Standard manipulations,[10] generalized to include a variable viscosity,[17,18] allow to rewrite the linearized system into the following generalized Orr–Sommerfeld and Squire equations for, respectively, the normal velocity $\hat{v}(y)$ and vorticity $\hat{\omega}_y(y)$:

$$\begin{bmatrix}D^2-k^2 & 0\\ 0 & 1\end{bmatrix}\frac{\partial}{\partial t}\begin{Bmatrix}\hat{v}\\ \hat{\omega}_y\end{Bmatrix}=\begin{bmatrix}\mathcal{L}_{OS} & 0\\ -i\beta U' & \mathcal{L}_{SQ}\end{bmatrix}\begin{Bmatrix}\hat{v}\\ \hat{\omega}_y\end{Bmatrix}, \tag{3}$$

with

$$\mathcal{L}_{OS}=-i\alpha[U(D^2-k^2)-U'']+\nu_T(D^2-k^2)^2+2\nu_T'(D^3-k^2D)+\nu_T''(D^2+k^2), \tag{4}$$

$$\mathcal{L}_{SQ}=-i\alpha U+\nu_T(D^2-k^2)+\nu_T'D, \tag{5}$$

where D and $(\,')$ stand for $\partial/\partial y$ and $k^2=\alpha^2+\beta^2$.

IV. OPTIMAL GROWTH

The mean velocity profiles displayed in Fig. 1(b) are linearly stable[15] for all α and β so that infinitesimal perturbations decay after enough time. However, some perturbations can grow before decaying. The ratio $\|\hat{\mathbf{u}}(t)\|^2/\|\hat{\mathbf{u}}_0\|^2$, where $\|\,\|$ stands for the energy norm, quantifies the energy amplification of a perturbation as it evolves in time. The temporal optimal growth $\hat{G}(\alpha,\beta,t)=\sup_{\hat{\mathbf{u}}_0}\|\hat{\mathbf{u}}(t)\|^2/\|\hat{\mathbf{u}}_0\|^2$ gives the maximum energy amplification of a perturbation optimized over all possible initial conditions $\hat{\mathbf{u}}_0$. In the following, we focus on the maximum optimal growth $G_{\max}(\alpha,\beta)$ $=\sup_t\hat{G}(\alpha,\beta,t)$ attained at the time $t_{\max}$ using the optimal initial conditions. The methods applied here to compute the maximum growth are the standard ones used in case of laminar flows and are easily extended to flows implying a variable viscosity $\nu_T^+(\eta)$. The operators $\mathcal{L}_{OS}$ and $\mathcal{L}_{SQ}$ are discretized using a spectral collocation method involving differentiation matrices[21] based on Chebyshev polynomials on a grid of N_y+1 collocation points. The numerical code has been validated in previous studies.[22] The results presented in this paper have been obtained using from 129 to 513 collocation points. We ensured the convergence of the results by checking that they were not modified when the number of collocation points was doubled.

Like in previous studies,[12,15] it is found that only structures elongated in the streamwise direction (i.e., with $\alpha\lesssim\beta$) are amplified and that the largest energy amplifications are reached by streamwise uniform (i.e., α=0) structures. We have, therefore, computed the optimal energy growths for several Reynolds numbers ranging from Re_τ=500 to Re_τ =20 000 considering only streamwise independent perturbations; essentially the same results are found for small streamwise wavenumbers ($\alpha h\lesssim 0.1$). From Fig. 2, where the curves $G_{\max}(\alpha=0,\beta)$ are reported for all Reynolds numbers considered, the typical[15,16] inner and outer peaks are readily seen. In accordance with what was found in Ref. 15, for spanwise wavelengths λ_z in between the two peaks, the time on which the maximum amplification is attained is found to be roughly proportional to λ_z. However, the maximum growth corre-

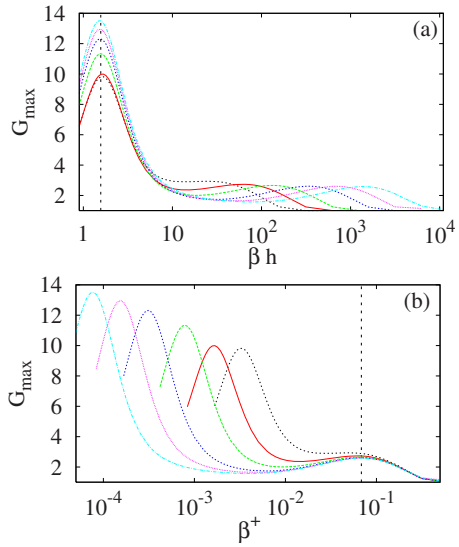

FIG. 2. (Color online) Maximum growth G_{max} of streamwise uniform ($\alpha=0$) perturbations for the Reynolds numbers $Re_\tau=500$, 1000, 2000, 5000, 10 000, and 20 000 as a function of the spanwise wavenumber in (a) outer units βh with a vertical dotted line at the optimal spanwise wavenumber $\beta h=1.5707$ corresponding to a spanwise wavelength $\lambda_z=4h$, (b) inner units β^+ with a vertical dotted line at the optimal spanwise wavenumber $\beta^+=0.0683$, corresponding to a spanwise wavelength $\lambda_z^+=92$ wall units. Same line styles as in Fig. 1.

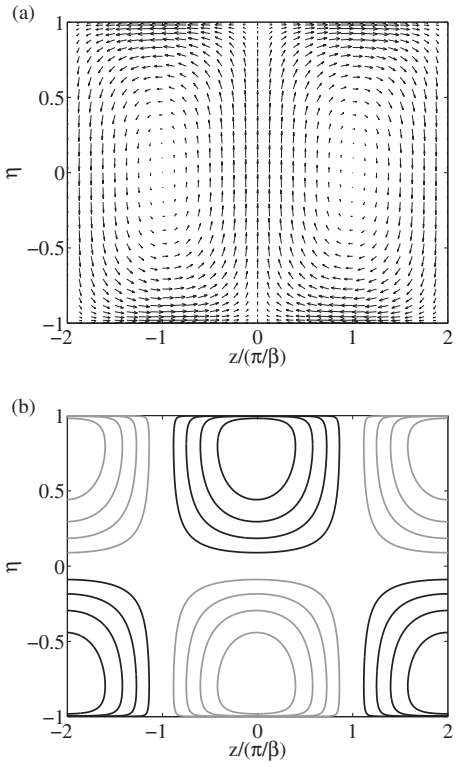

FIG. 3. Transverse view of the optimal solution corresponding to the primary peak ($\lambda_z=4h$) for $Re_\tau=5000$: (a) represents the initial (v,w) field ($t=0$); (b) represents the optimal streamwise velocity streaks obtained in response to this perturbation at $t=t_{max}$. The black contours are high velocity streaks $u>0$ and the gray contours are low velocity streaks $u<0$. The levels are 0.2(+0.2)0.8.

sponding to the main peak is found to increase with the Reynolds number, contrary to what was found in Ref. 15. A cross-stream view of the optimal perturbations corresponding to the outer peak is reported in Fig. 3. The optimal initial condition consists in counter-rotating streamwise vortices filling the whole channel and inducing, optimally amplified streamwise velocity streaks of spanwise alternating signs, each streak filling half channel depth. The structures associated with the secondary peaks also consist in optimal initial vortices and final streaks and are in very good agreement with previous results[15] and are not reported here.

V. SCALING WITH THE REYNOLDS NUMBER

A. Scaling of the maximum growth

From Fig. 2(b), it is seen that the data obtained at different Reynolds numbers and corresponding to the secondary peak collapse on a single curve if they are scaled in inner units and the Reynolds number is sufficiently large (roughly larger than $Re_\tau\sim4000$ according to our computations). This is consistent with what was found by del Álamo and Jiménez,[15] even if the precise values of the peak slightly differ. In particular, the maximum growth $G_{max}^{(inn)}=2.6$ (less than the ~3.5 found in Ref. 15) is obtained for $\beta^+=0.0683$, corresponding to a spanwise wavelength of $\lambda_z^+=92$ wall units. The time $t_{max}^+=t_{max}u_\tau^2/\nu$ at which the maximum growth is attained roughly ranges from 19 to 16 slightly decreasing with Re_τ. The fact that the maximum growth corresponding to inner scaling structures is almost independent of Re_τ has been qualitatively explained in Ref. 15 by showing that the Reynolds number typical of these most amplified inner structures is close to constant and very low (of the order of ten).

The primary peak $G_{max}^{(out)}$ is attained, for the considered set of Re_τ, at $\beta h=1.5707$ corresponding to an optimal spanwise wavelength $\lambda_z=4h$ (a value slightly larger than the $\sim3h$ value found in Refs. 12 and 15). The maximum energy growth is of the order of ten and increases with Re_τ (see Fig. 2). In the laminar channel flow case the maximum energy growth scales with the square of the Reynolds number[11,23,24] based on the center line velocity U_e, half-channel width h and the molecular viscosity. In the present turbulent case, therefore, we try a scaling with an "effective" turbulent Reynolds number $Re_\bullet=U_eh/\nu_{T_{max}}$ based on the outer units h, U_e and the maximum total viscosity $\nu_{T_{max}}=\sup_y \nu_T(y)$. This outer-unit-effective Reynolds number should not be confused with the effective Reynolds number defined in Ref. 15 associated with inner layer structures and used to interpret the inner peak growth. For the considered mean flow profiles, $Re_\bullet$ ranges from 256 to 368 when Re_τ is between 500 and 20 000. The maximum energy amplification $G_{max}^{(out)}$ is seen to scale approximately linearly with $Re_\bullet$. In Fig. 4(a) $G_{max}^{(out)}$ and its fit $0.037\,87\ Re_\bullet$ are plotted versus Re_τ. The optimal dimensionless time $t_{max}U_e/h$ at which the outer peak optimal is attained increases with the Reynolds number scaling approximately like $Re_\bullet^{3/2}$ [see Fig. 4(b)]. As presently there is no theoretical support for these scalings, they should be considered only as empirical data fits. Furthermore, for large Reynolds numbers ($Re_\tau\geq10\,000$) the $G_{max}^{(out)}$ curve begins to deviate from the linear behavior in $Re_\bullet$ (and it deviates even

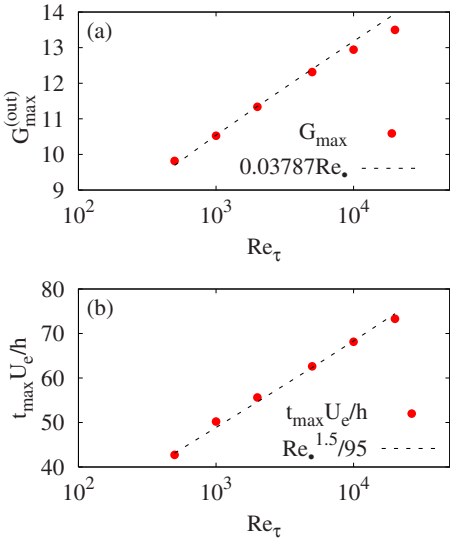

FIG. 4. (Color online) (a) Maximum growth $G_{max}^{(out)}$ corresponding to the outer peak vs Re_τ. The dashed line is the fit 0.037 87 Re_τ. (b) Associated dimensionless time vs Re_τ. The dashed line is the fit $Re_\tau^{3/2}/95$.

further for larger Re_τ). However, we have to remind that the κ and A constants used to fit the eddy viscosity and the mean profile have been calibrated versus DNS at the low $Re_\tau=2000$, and therefore, probably no conclusions can be drawn at very large Re_τ.

B. Scaling of the optimal perturbations

In Fig. 5, the wall normal velocity component v of the initial vortices and the streamwise velocity component u of the resulting streaks for each Reynolds number are plotted versus, respectively, the wall normal inner (y^+) and outer (η)

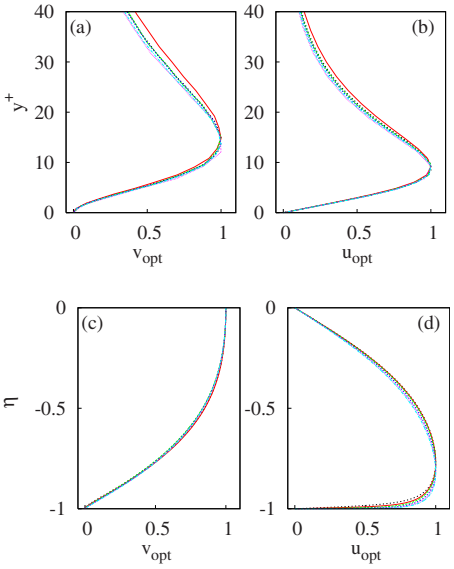

FIG. 5. (Color online) [(a) and (c)] Normalized amplitude of the v component of the optimal initial vortices and [(b) and (d)] of the u component of the corresponding optimally amplified streaks for $Re_\tau=500$, 1000, 2000, 5000, 10 000, and 20 000 (recall that for $\alpha=0$, u and v are real while w is pure imaginary). [(a) and (b)] Corresponding to the secondary peak in Fig. 2, displayed in wall units. [(c) and (d)] Corresponding to the main peak in Fig. 2, displayed in outer units. Same line styles as in Fig. 1.

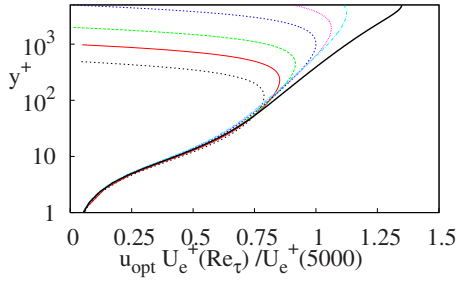

FIG. 6. (Color online) Normalized u component of the optimally amplified streaks corresponding to the main peak. Same data as in Fig. 5(d) but in wall units and normalized with the $Re_\tau=5000$ case. Line styles as in Fig. 1. The solid line represents the mean flow profile corresponding to $Re_\tau=5000$ and normalized with an arbitrary constant to match the normalization of the optimal streaks (only half channel represented here).

coordinates. The optimal perturbations are seen to assume a shape almost independent of the Re_τ when rescaled in proper units, even if this independence is only qualitative, as revealed by a close examination of Fig. 5. Regarding the inner peak, it is observed that the maximum of the optimal initial v, giving the distance from the wall of the optimal initial counter-rotating vortices, is situated approximately at $y^+=15$, while the maximum of the optimal final u is situated near $y^+=10$. As for the outer peak, the maximum of the optimal initial v is located at the channel center $\eta=0$ while the maximum of optimal outer streak is situated near the wall, at $|\eta|=0.80$.

When replotted in inner variables, the amplitudes of the outer optimal streaks collapse on a single curve in the log and near wall regions where they are proportional to the mean flow velocity profile U. This is shown in Fig. 6 where the data already reported in Fig. 5(d) are replotted in inner variables expressing u_{opt} in wall units by using the factor $U_e^+(Re_\tau)/U_e^+(5000)$ where $Re_\tau=5000$ is taken as the reference case. In the same figure, the $Re_\tau=5000$ mean velocity profile rescaled to have unit amplitude at the position of the maximum of the corresponding streak (where the streak amplitude is also normalized to one) is also reported for comparison. This particular scaling of the optimal streaks allow them to have very large amplitudes inside the near wall region, just like the mean flow: at $y^+=10$, they can still have half of their maximum amplitude.

VI. SUMMARY AND DISCUSSION

The computation of the optimal energy growth in a turbulent channel flow by del Álamo and Jiménez[15] has been repeated using a linear operator consistent with previous investigations of laminar[18] or turbulent[17] flows with variable eddy viscosity.

As in Ref. 15, and consistently with the analogous analysis of a turbulent boundary layer,[16] it is found that: (a) only streamwise elongated structures can be transiently amplified; (b) the most amplified perturbations are streamwise uniform and consist in streamwise vortices amplified into streamwise streaks; (c) for sufficiently large Reynolds numbers two different peaks of the optimal growth $G_{max}(\alpha=0,\beta)$ are found, scaling in inner and in outer units, respectively; (d) the maxi-

mum growth associated with the inner peak does not depend on Re_τ and is obtained for structures having a spanwise wavelength $\lambda_z^+ \approx 100$; and (e) the time at which the optimals are reached is roughly proportional to their spanwise wavelength λ_z.

The optimal spanwise wavenumber ($\lambda^+=92$) and growth ($G_{\max}^{(\mathrm{inn})}=2.6$) corresponding to the peak scaling in inner units are slightly smaller that the ones found in Ref. 15, and the difference must be attributed to the different linear operators used in the analysis. The precise figures of these optimal values should not, however, be overemphasized because of the very crude assumptions made in their derivation and because their value slightly depends also on the choice of the von Kármán κ and A constants used for the mean flow fits. The selected optimal λ_z^+ are anyway in very good accordance with experimental results[1,2] where the measured mean spacing of near wall streaks ranges from 80 to 110 in an apparently random way.

The most important difference with the results obtained in Ref. 15 is that the maximum growth corresponding to the outer peak increases with the Reynolds number. In a first approximation, the outer optimal growth scales linearly with an effective turbulent Reynolds number based on outer units, similar to what is observed for the turbulent boundary layer.[16] The optimal growth is obtained for structures with a spanwise wavelength $\lambda_z \sim 4h$, larger than the laminar optimal, which is also consistent with what is found in the turbulent boundary layer case.[16]

The optimal vortices and streaks corresponding to the two peaks are seen to be approximately self-similar in respective inner and outer units. The optimal streaks corresponding to the outer peak are, however, seen to scale also in inner units in the viscous layer (roughly $y^+ \lesssim 150$), where they are proportional to the local mean velocity. The outer streaks have, therefore, non-negligible amplitudes in all the viscous layer (they have up to 50% of their maximum amplitude near $y^+=10$).

The two combined facts that the outer peak $G_{\max}^{(\mathrm{out})}$ increases with Re_τ and that the associated optimal streaks strongly protrude into the viscous layer, can be related to experimental and numerical evidence of the influence of outer scales into the inner layers. In particular, it has been observed both in experiments[25] and numerical simulations[20] that the streamwise turbulent intensity u_{rms} in the outer layer of wall flows does not collapse in wall units with increasing Re_τ and that this lack of collapse grows with Re_τ.

Structures almost streamwise uniform ($\lambda_x \gg h$) with $\lambda_z \sim 4h$ are observed in DNS of turbulent channel flows[6] even if these structures are not the most energetic ones. The observed most energetic structures are not streamwise uniform but have finite λ_x typical of the order of $\approx 5-10h$ (corresponding to $\alpha h \approx 0.5-1$) and a typical spacing $\lambda_z \approx 2-3h$, which corresponds well to the optimal λ_z that would be found for those α (e.g., for $\alpha h=1$ the optimal is $\lambda_z=2.45$). The fact that the streamwise uniform streaks are not the most energetic ones probably means that these structures are not self-sustained or are only weakly sustained because of a poor feedback to reform the vortices or that they are just passively forced by other self-sustained structures. This is because the amplification of the streaks is only part of more complex processes leading, e.g., to self-sustained cycles. To see these potentially largely amplified structures, one must probably artificially force them as recently done in the turbulent Couette flow.[26] Forcing large amplitude streaks could be interesting to manipulate the flow, as already shown in the case of laminar boundary layers.[27,28]

ACKNOWLEDGMENTS

We are pleased to acknowledge fruitful discussions with J. Jiménez and J. C. del Álamo. G.P. acknowledges partial support from ANRT through a "Convention CIFRE." M.G.-V. acknowledges the financial support of the German Research Foundation (DFG) through the project GA1360/2-1.

[1] S. J. Kline, W. C. Reynolds, F. A. Schraub, and P. W. Runstadler, "The structure of turbulent boundary layers," J. Fluid Mech. **30**, 741 (1967).
[2] J. R. Smith and S. P. Metzler, "The characteristics of low-speed streaks in the near-wall region of a turbulent boundary layer," J. Fluid Mech. **129**, 27 (1983).
[3] L. S. G. Kovasznay, V. Kibens, and R. F. Blackwelder, "Large-scale motion in the intermittent region of a turbulent boundary layer," J. Fluid Mech. **41**, 283 (1970).
[4] N. Hutchins and I. Marusic, "Evidence of very long meandering features in the logarithmic region of turbulent boundary layers," J. Fluid Mech. **579**, 1 (2007).
[5] J. Komminaho, A. Lundbladh, and A. V. Johansson, "Very large structures in plane turbulent Couette flow," J. Fluid Mech. **320**, 259 (1996).
[6] J. C. del Álamo and J. Jiménez, "Spectra of the very large anisotropic scales in turbulent channels," Phys. Fluids **15**, L41 (2003).
[7] H. K. Moffatt, "The interaction of turbulence with strong wind shear," in *Proceedings of the URSI-IUGG Colloquium on Atoms, Turbulence and Radio Wave Propagation*, edited by A. M. Yaglom and V. I. Tatarsky (Nauka, Moscow, 1967), pp. 139–154.
[8] T. Ellingsen and E. Palm, "Stability of linear flow," Phys. Fluids **18**, 487 (1975).
[9] M. T. Landahl, "A note on an algebraic instability of inviscid parallel shear flows," J. Fluid Mech. **98**, 243 (1980).
[10] P. J. Schmid and D. S. Henningson, *Stability and Transition in Shear Flows* (Springer, New York, 2001).
[11] K. M. Butler and B. F. Farrell, "Three-dimensional optimal perturbations in viscous shear flow," Phys. Fluids A **4**, 1637 (1992).
[12] K. M. Butler and B. F. Farrell, "Optimal perturbations and streak spacing in wall-bounded turbulent shear flow," Phys. Fluids A **5**, 774 (1993).
[13] W. C. Reynolds and W. G. Tiederman, "Stability of turbulent channel flow, with application to Malkus's theory," J. Fluid Mech. **27**, 253 (1967).
[14] R. D. Cess, "A survey of the literature on heat transfer in turbulent tube flow," Research Report No. 8-0529-R24, Westinghouse, 1958.
[15] J. C. del Álamo and J. Jiménez, "Linear energy amplification in turbulent channels," J. Fluid Mech. **559**, 205 (2006).
[16] C. Cossu, G. Pujals, and S. Depardon, "Optimal transient growth and very large scale structures in turbulent boundary layers," J. Fluid Mech. **619**, 79 (2009).
[17] W. C. Reynolds and A. K. M. F. Hussain, "The mechanics of an organized wave in turbulent shear flow. Part 3. Theoretical models and comparisons with experiments," J. Fluid Mech. **54**, 263 (1972).
[18] F. M. White, *Viscous Fluid Flows*, 3rd ed. (McGraw-Hill, New York, 2006).
[19] In Ref. 15, the eddy viscosity is defined using $\hat{\eta}$ defined in the domain [0,2] with $\hat{\eta}=\eta+1$. Even if the correct expression seems to have been used, some misprints appear in Eq. (2.2) of Ref. 15, that should read instead: $\nu_T(\hat{\eta})=(1/2)\{1+(\kappa^2\,\mathrm{Re}_\tau^2/9)(2\hat{\eta}-\hat{\eta}^2)^2(3-4\hat{\eta}+2\hat{\eta}^2)^2\{1-\exp[(|\hat{\eta}-1|-1)\mathrm{Re}_\tau/A]\}^2\}^{1/2}+(1/2)$.
[20] S. Hoyas and J. Jiménez, "Scaling of the velocity fluctuations in turbulent channels up to $\mathrm{Re}_\tau=2003$," Phys. Fluids **18**, 011702 (2006).
[21] J. A. C. Weideman and S. C. Reddy, "A MATLAB differentiation matrix suite," ACM Trans. Math. Softw. **26**, 465 (2000).

[22]E. Lauga and C. Cossu, "A note on the stability of slip channel flows," Phys. Fluids **17**, 088106 (2005).
[23]L. H. Gustavsson, "Energy growth of three-dimensional disturbances in plane Poiseuille flow," J. Fluid Mech. **224**, 241 (1991).
[24]S. C. Reddy and D. S. Henningson, "Energy growth in viscous channel flows," J. Fluid Mech. **252**, 209 (1993).
[25]D. B. De Graaff and J. K. Eaton, "Reynolds-number scaling of the flat-plate turbulent boundary layer," J. Fluid Mech. **422**, 319 (2000).
[26]O. Kitoh and M. Umeki, "Experimental study on large-scale streak structure in the core region of turbulent plane Couette flow," Phys. Fluids **20**, 025107 (2008).
[27]C. Cossu and L. Brandt, "Stabilization of Tollmien–Schlichting waves by finite amplitude optimal streaks in the Blasius boundary layer," Phys. Fluids **14**, L57 (2002).
[28]J. Fransson, A. Talamelli, L. Brandt, and C. Cossu, "Delaying transition to turbulence by a passive mechanism," Phys. Rev. Lett. **96**, 064501 (2006).